U.P.B. Sci. Bull., Series B, Vol. 78, Iss. 3, 2016 ISSN 1454-2331

OPTICAL PROPERTIES OF PYROSOL SYNTHESIZED TiO_2 NANOSTRUCTURES

Otilia – Ruxandra VASILE[1], Ecaterina ANDRONESCU[2], Roxana TRUSCA[3], Ovidiu OPREA[4], Eugeniu VASILE[5], Bogdan Stefan VASILE[6]*

The aim of the current study was the synthesis and characterization of TiO_2 nanostructured powders by pyrosol method, together with characterization and optical properties characterization. A diluted solution of $TiCl_3$ 0.1 M was used as starting precursor and the synthesis temperatures used were in range of 400 – 600°C. The obtained nanostructured powders were characterized by X-ray diffraction, Scanning and transmission electron microscopy. The results showed that the synthesized TiO_2 nanostructured particles exhibit strong luminescence under 320 nm excitation, a high absorbance in UV region and almost no photocatalytic activity. Such nanostructured particles are the best candidates for textile industry or cosmetic industry, where the usual photocatalytic activity of TiO_2 is a major drawback.

Keywords: TiO_2, cytotoxicity, pyrosol method, nanostructures, synthesis

1. Introduction

Due to its high activity, TiO_2 nanoparticles are the most used materials for photocatalytic applications [1, 2]. TiO_2 is capable of a wide variety of applications in industry, medicine and life sciences, due to its properties, such as high chemical stability, non-toxicity and low cost in addition to high activity [3, 4, 5] as well. TiO_2 is stable from the chemical point of view and is considered relatively nontoxic [6].

TiO_2 is important in a wide range of applications, such as paints and cosmetics due to its strong white colour, and also in photochromism, solar

[1] Scientific Researcher, Dept. of Science and Engineering of Oxide Materials and Nanomaterials, University POLITEHNICA of Bucharest, Romania, e-mail: otilia.vasile@upb.ro
[2] Prof., Dept. of Science and Engineering of Oxide Materials and Nanomaterials, University POLITEHNICA of Bucharest, Romania, e-mail: ecaterina.andronescu@upb.ro
[3] METAV - CD, Bucharest, Romania, e-mail: truscaroxana@yahoo.com
[4] Prof., Dept. of Science and Engineering of Oxide Materials and Nanomaterials, University POLITEHNICA of Bucharest, Romania, e-mail: ovidiu73@yahoo.com
[5] Scientific Researcher, Dept. of Science and Engineering of Oxide Materials and Nanomaterials, University POLITEHNICA of Bucharest, Romania, e-mail: eugeniu.vasile@upb.ro
[6] Scientific Researcher, National Research Center for Micro and Nanomaterials, and Dept. of Science and Engineering of Oxide Materials and Nanomaterials, University POLITEHNICA of Bucharest, Romania, e-mail: bogdan.vasile@upb.ro

applications [7, 8, 9], self-cleaning [10, 11], micro chemical systems, gas sensors [12], anti-fogging, water splitting, water purification [13], air purification [14], lithography, sterilisation, degradation of organic compounds, artificial photosynthesis, and metal corrosion prevention.

TiO_2 nanoparticles are also used in textiles industry as a UV blocking filter to protect the fabric from the harmful radiation. One problem that limits this application is the photocatalytic activity of TiO_2, which is high enough to degrade overtime the same fabric that was meant to protect. Another side effect that appear by wearing such treated cloths or by using cosmetics which contains TiO_2 is the possible uptake of nanoparticles through skin cells [15].

Titanium dioxide occurs in nature in different crystalline forms: anatase, rutile and brookite [16]. Anatase is the most photoactive phase and rutile is thermodynamically the most stable. Anatase and rutile crystal lattices are composed of chains of octahedral TiO_2, with different connectivity [17]. The stability of various TiO_2 crystalline forms are also size dependent [18]. To improve the photocatalytic activity, combining TiO_2 with various materials can be used in order to obtain composites with better photocatalytic efficiency [4].

Due to the expression of relatively low energy surfaces, anatase is actually the most stable TiO_2 structure for nanometric sizes and can be prepared using various low temperature syntheses methods [19]. Experimental conditions variation gave rise to a multitude types of nanoparticles morphologies, starting from rods, classical truncated square bipyramids, needles, cubes, squares plates, belts, etc. A clear correlation between particles morphology and photocatalytic efficiency is not completely understood.

Pyrosol synthesis method has been chosen for TiO_2 synthesis in order to achieve fine TiO_2 nanostructured materials and homogeneous dispersion at the nanometer level [20, 21, 22].

The aim of the present study is to provide a detailed correlation between the photocatalytic efficiency of different TiO_2 nanostructures on the same photocatalytic test and their synthesis temperature. Pyrosol syntheses [23, 24, 285, 26, 27] were used to prepare TiO_2 nanoparticles in synthesis temperatures in range of 400°C and 600°C. The main focus was on synthesis and complete characterization of pyrosol synthesized TiO_2 nanostructures in mentioned synthesis temperatures range, as well as photocatalytic properties determination.

In order to elucidate the real impact of synthesis temperature on photocatalytic activity, a fine characterization of TiO_2 nanostructured particles was achieved using high-resolution transmission electron microscopy analysis. The photocatalytic efficiencies of the selected samples for the degradation of the rhodamine B dye under UV light are presented [28].

In this paper we report for the first time to our knowledge the synthesis of TiO_2 nanostructured particles, anatase phase, with negligible photocatalytic activity, but with high UV absorbance, properties that makes them suitable as UV shields in various applications.

2. Experimental procedure

2.1 Synthesis of TiO_2 powders

TiO_2 powders have been synthesized using pyrosol method, according to previously reported studies [20, 29, 30, 31, 32]. Through this method, we can easily obtain dense and round nanostructured particles, with dimensions in range of 10 – 1000 nm.

TiO_2 powders synthesis has been done starting from a diluted precursor solution of $TiCl_3$ (Sigma Aldrich) with a concentration of 0.1 M and the synthesis temperatures of 400°C, 500°C and 600°C respectively.

2.2 Characterization of TiO_2 nanoparticles

The synthesized nanostructured powders have been characterized from the compositional, morphological and structural point of view by using analysis such as X-ray diffraction analysis (XRD), scanning electron microscopy (SEM) and transmission electron microscopy (TEM), and optical properties respectively.

XRD analysis was carried out on Panalytical X'Pert Pro MPD equipment, with a Cu K_a radiation. The SEM analysis was carried out by using a Quanta Inspect F microscope from FEI Company with field emission gun (FEG) and a 1.2 nm resolution. The Bright Field and HIGH Resolution Images Coupled with SAED were obtained using a Tecnai G^2 F30 S-TWIN transmission electron microscope.

Absorption spectra were recorded with a JASCOV560 spectrophotometer with solid sample accessory, in the range of 200– 850 nm, with a speed of 200 nm min^{-1}.

The photoluminescence spectrum (PL) of the TiO_2 samples (in solid state) were recorded with a Perkin Elmer P55 spectrometer using a Xe lamp as a UV light source at ambient temperature, in the range 200-800 nm. An excitation wavelength of 320 nm was used.

Photocatalytic activity was measured against methylene blue (MB) solution, 10^{-4}%, by irradiation with an Hg fluorescence lamp. Samples of TiO_2 nanopowder (0.0220 g) were introduced in 20 mL solution of MB. At defined intervals of time (of 1-4 h) a 2 mL of sample of were taken out and its UV-Vis spectra was recorded. The maximum absorption of MB solutions, 664 nm, was used for data interpretation.

3. Results and discussion

3.1 X-ray diffraction characterization

TiO_2 nanostructured powders synthesized through pyrosol at synthesis temperatures in range of 400 – 600°C have been characterized from the phase composition point of view by using X-ray diffraction analysis, the obtained spectra being presented in Fig. 1.

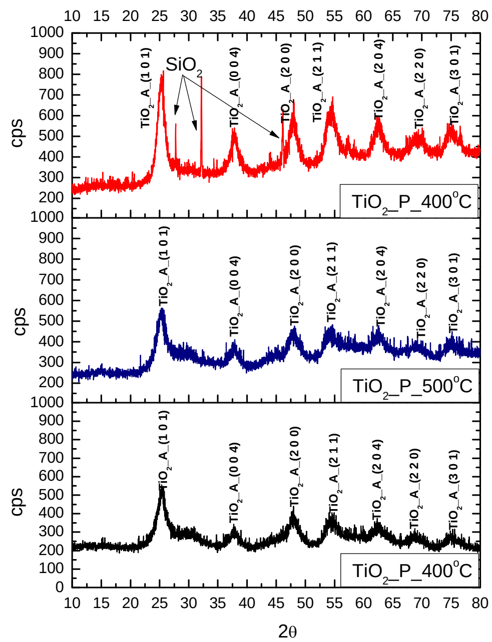

Fig. 1. XRD patterns for TiO_2 nanostructured powders synthesized through pyrosol method at 400°C, 500°C, 600°C

By analysing XRD spectra obtained on TiO_2 powders synthesized through pyrosol method, it could be seen that for all synthesis temperatures we can identify the anatase polymorph phase of TiO_2 [ASTM 01-070-6826] [33].

In table 1 is presented the average crystallite size variation against the synthesis temperature, for pyrosol synthesized TiO_2 powders.

Table 1

Average crystallite size variation with synthesis temperature obtained on TiO_2 powders synthesized through pyrosol method

Temperature (°C)	Average crystallite size (nm) Pyrosol synthesis
400	3.8
500	4.6
600	6.0

All crystallite size values have been obtained by using Scherer's formula and varies in range of 3.8 – 6 nm.

3.2 Scanning electron microscopy analysis

SEM images obtained for TiO_2 powders synthesized through pyrosol method at 400°C, 500°C and 600°C, are presented in Fig. 2.a-c.

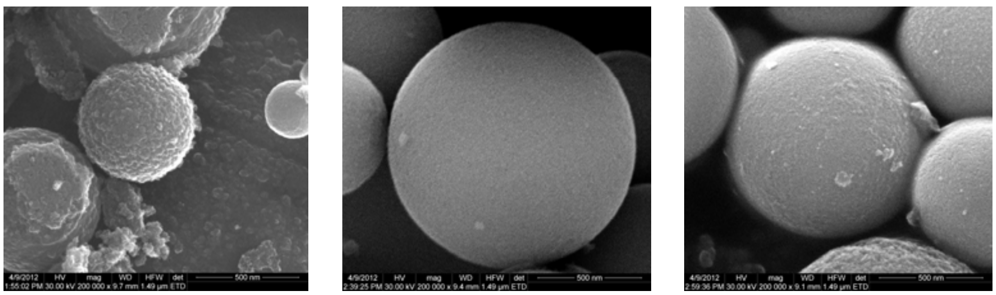

a) b) c)

Fig. 2. SEM images for TiO_2 powders synthesized through pyrosol method at 400°C, a), 500°C, b) and 600°C, c), starting from precursor solution of 0.1 M

SEM images for TiO_2 powders synthesized through pyrosol method at 400°C, 500°C, and 600°C, starting from a precursor solution of 0.1 M, presents powders with spherical morphology and homogeneous from dimensional point of view. The size of the particles varies between 0.4 μm to 1 μm for all three used synthesis temperatures.

At 400°C, it could be seen that powder is not so well formed, presenting some irregularities on the surfaces.

3. 3 Transmission electron microscopy analysis

Transmission electron microscopy images in bright field, as well as high-resolution transmission electron microscopy obtained on TiO_2 powders synthesized through pyrosol method at synthesis temperatures in range of 400°C - 600°C, are presented in Fig. 3.

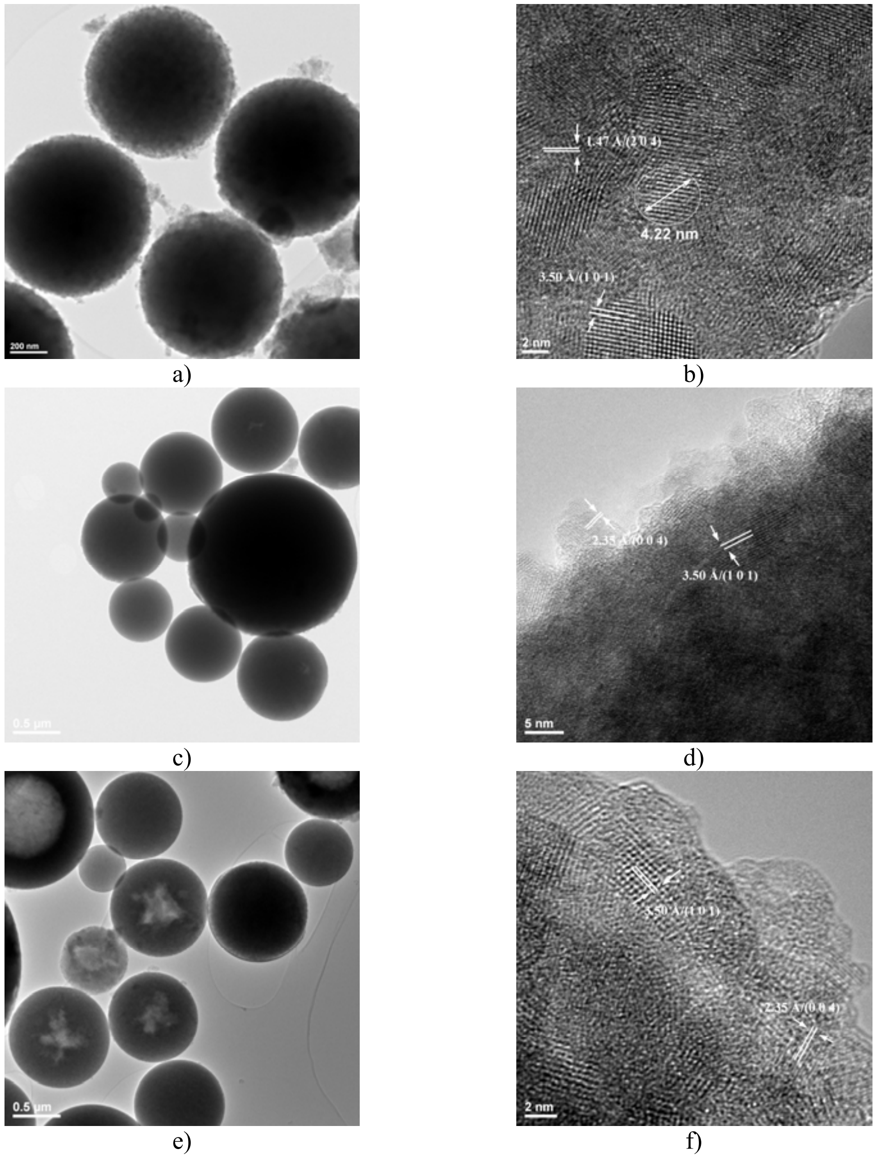

Fig. 3. BF-TEM images for TiO_2 powders synthesized through pyrosol method at 400°C, a), 500°C, c) and 600°C, e), respectively HRTEM corresponding images (b, d, f) starting from 0.1 M precursor concentration of solution

Bright field transmission electron microscopy images obtained on TiO_2 nanostructures presents round particles that in fact are agglomerates of nanocrystallites. The crystallites that are inside the agglomerates have dimensions in the range of 3 to 5 nm, this being evidenced in HRTEM images.

HRTEM images are presenting polycrystalline nanostructures, well crystallized for all synthesis temperatures, from which could be distinguished structures with atomic planes families that have Miller indices orientations (101), (004) and (204), corresponding to interplanar distances of d = 3,50 Å, d = 2,35 Å and d = 1,47 Å of anatase phase of TiO_2. The values obtained from the measuring crystallites from TEM are almost the same with the ones calculated from XRD data.

4. Optical properties

4.1 Photoluminescence spectroscopy

Photoluminescence spectra corresponding to powders synthesized through pyrosol method (Fig. 4), are indicating a significant decrease of blue-green emission, as synthesis temperature is increasing (intensity of emission bands is decreasing to half by increasing the synthesis temperature from 400°C to 600°C).

This behavior can have two possible causes. The first explanation is based on possible presence of HO^- groups on surface of the synthesized nanostructured particles at lower temperature. The presence of HO^- groups on surface of the nanostructured particles is enhancing the fluorescent emission [34, 35, 36], by blocking of the nonradiative recombination centers on the surface and the nonradiative transition paths. While these groups are eliminated by increasing synthesis temperature, intensity of fluorescent emission is decreasing.

A second explanation for fluorescent emission intensity decreasing is that the nanostructures obtained at 500°C and 600°C have a higher density of defects generated by the increased temperature. This multitude of the defects and type of defects represents new recombination centers for the electrons or holes, inducing the quenching of fluorescent emission.

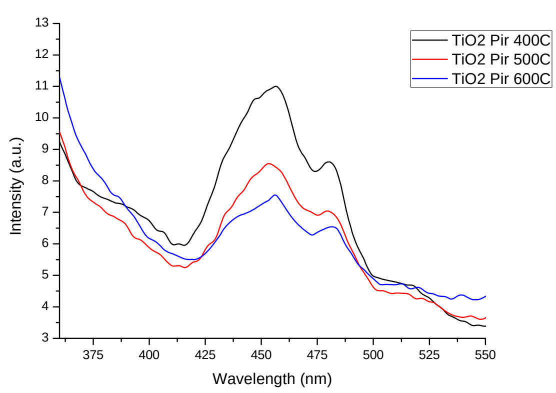

Fig. 4. Emission spectra for TiO_2 nanostructures obtained through pyrosol method

4.2 UV-Vis spectroscopy

UV-Vis spectra for TiO_2 nanostructures synthesized through pyrosol method at synthesis temperatures of 400°C, 500°C and 600°C is presented in Fig. 5,while the determination of the band-gap energy by Tauc method is presented in Fig. 6.

The electronic spectra present a shift of absorption maxima from 334 nm (400^{o}C) to 358 nm (600°C) (Fig. 5). In visible range, it can be seen the existence of an extended absorption band for entire range, while the intensity is increasing with the increase of synthesis temperature. This confirms our earlier supposition that for the lower temperatures samples there is still a fair amount of HO^- groups on the surface.

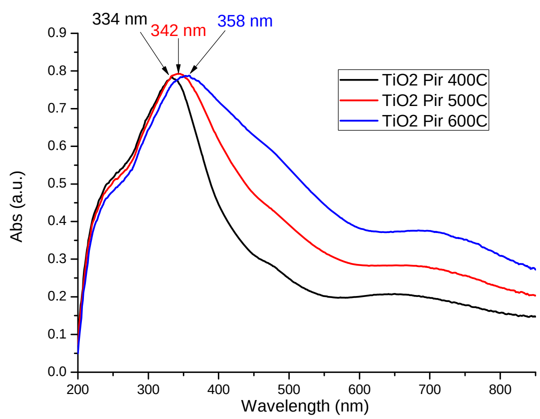

Fig. 5. Electronic spectra for TiO_2 nanostructures obtained through pyrosol method

For TiO_2 nanostructure synthesized through pyrosol method at 400°C, the calculated bad-gap energy of 3.26 eV is very close to the theoretical value of 3.2 eV.

For TiO_2 nanostructures synthesized through pyrosol method at 500°C and 600^{o}C, the calculated band-gap energy is lower. One explanation is that small quantities of rutile is formed at higher temperatures, but are quantitatively insufficient for XRD detection. These rutile impurities are generating new, intermediary electronic levels, leading to a small decrease of the band-gap values.

A second explanation is the generation of intermediary electronic levels by network defects. As nanoparticles synthesis is done at higher temperature, in a very short time (specific to this synthesis method), the presence of a multitude of network defects is generating intermediary electronic levels in forbidden band. While synthesis temperature is increasing, the reaction for TiO_2 synthesis is more violent, and the possibility of inducing network defects increases.

The tail which appears in visible range of the electronic spectra (Fig. 5) could be seen as an extended absorption band which becomes more intense as synthesis temperature increases. This extended band in visible range can be easily explained through acceptance of more types of defects in crystalline network. The defects induce possibility of existence for more types of electronic transitions, and finally to the presence of an extended absorption band.

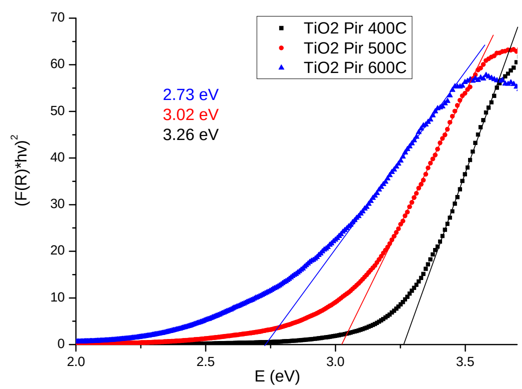

Fig. 6. Tauc graph of modified Kubelka Munk function versus photon energy, for forbidden band energy determination for TiO_2 nanostructures synthesized through pyrosol method for all synthesis temperatures

4.3 Photocatalytic activity

The photocatalytic determinations for all three samples obtained at temperatures between 400 - 600°C indicate that the TiO_2 nanopowders, despite anatase structure, present no activity (Fig. 7). To our knowledge is the first time such behavior is reported.

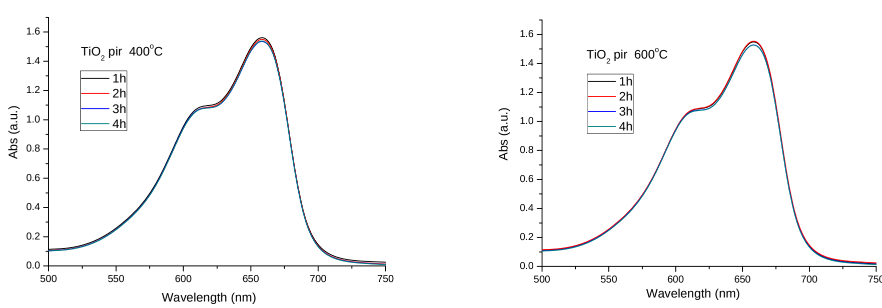

Fig. 7. Photocatalytic activity for the TiO_2 nanostructures obtained through pyrosol method

We attributed this behaviour to the solid spherical morphology obtained during the synthesis. This unique solid nanostructure, with hundreds of crystallite on each particle, results in lower separation efficiency of photogenerated electrons and holes in the TiO_2 nanocrystals and such to a very low photocatalytical activity.

5. Conclusions

In conclusion we have prepared and characterized TiO_2 nanopowders by pyrosol method in the temperature range of 400 - 600^{o}C. The nanoparticles have a solid spherical morphology, with the diameter of about 500 nm but with crystallite size of ~4 nm. The optical properties indicate a good absorbance in UV-Vis domains and high luminescence emission. We report here for the first time to our knowledge the obtaining of TiO_2 nanoparticles, anatase phase, with negligible photocatalytic activity that makes them suitable as UV shield in various applications as textile coating or cosmetic industry.

Acknowledgement

This paper is supported by the Sectorial Operational Program Human Resources Development, financed from the European Social Fund, and by the Romanian Government under the contract number ID 134398 (KNOWLEDGE). Also the SEM analyzes on the samples were possible due to EU-funding grant POSCCE-A2-O2.2.1-2013-1/Priority axe 2, Project No. 638/12.03.2014, code SMIS-CSNR 48652. The XRD measurements were possible due to EU-funding grant financed from the Sectoral Operational Programme Human Resources Development, European Social Fund, and by the Romanian Government under the contract number POSDRU/86/1.2/S/ 58146 (MASTERMAT)".

R E F E R E N C E S

[1] *C. Guild, S. Biswas, Y. Meng, T. Jafari, A.M. Gaffney, S.L. Suib*, Perspectives of spray pyrolysis for facile synthesis of catalysts and thin films: An introduction and summary of recent directions, Catalysis Today, **vol. 238**, 2014, pp. 87–94

[2] *O. Arutanti, A. Bayu, D. Nandiyanto, T. Ogi, F. Iskandar, T.O. Kim, K. Okuyama,* Synthesis of composite WO3/TiO2 nanoparticles by flame-assisted spray pyrolysis and their photocatalytic activity, Journal of Alloys and Compounds, **vol. 591**, 2014, pp. 121–126

[3] *L. Pan, X. Zhang, L. Wang, J. Zou,* Controlling surface and interface of TiO2 toward highly efficient, Photocatalysis, Materials Letters, 2015, doi:10.1016/j.matlet.2015.06.109

[4] *O. Ola, M.M. Maroto-Valer,* Review of material design and reactor engineering on TiO2 photocatalysis for CO2 reduction, Journal of Photochemistry and Photobiology C: Photochemistry Reviews, **vol. 24**, 2015, pp. 16–42

[5] *B. Grbić, N. Radić, S. Stojadinović, R. Vasilić, Z. Dohčević-Mitrović, Z. Šaponjić, P. Stefanov*, TiO2/WO3 photocatalytic composite coatings prepared by spray pyrolysis, Surface & Coatings Technology, **vol. 258**, 2014, pp. 763–771
[6] *M. Song, R. Zhang, Y. Dai, F. Gao, H. Chi, G. Lva, B. Chen, X. Wang*, The in vitro inhibition of multidrug resistance by combined nanoparticulate titanium dioxide and UV irradition, Biomaterials, **vol. 27**, 2006, pp. 4230–4238
[7] *M. Dudita, L.M. Manceriu, M. Anastasescu, M. Nicolescu, M. Gartner, A. Duta,* Coloured TiO2 based glazing obtained by spray pyrolysis for solar thermal applications, Ceramics International, **vol. 40**, 2014, pp. 3903–3911
[8] *I. Tantis, M.V. Dozzi, L.G. Bettini, G.L. Chiarello, V. Dracopoulos, E. Selli, P. Lianos*, Highly functional titania nanoparticles produced by flame spray pyrolysis. Photoelectrochemical and solar cell applications, Applied Catalysis B Environmental, doi:10.1016/j.apcatb.2015.09.040
[9] *C. Dwivedi, V. Dutta, A.K. Chandiran, K. Nazeeruddin, M. Grätzel,* Anatase TiO2 Hollow Microspheres Fabricated by Continuous Spray Pyrolysis as a Scattering Layer in Dye-Sensitised Solar Cells, Energy Procedia, **vol. 33**, 2013, pp. 223 – 227
[10] *W. Shen, C. Zhang, Q. Li, W. Zhang, L. Cao, J. Ye,* Preparation of titanium dioxide nano particle modified photocatalytic self-cleaning concrete, Journal of Cleaner Production, **vol. 87**, 2015, pp. 762-765
[11] *S. Banerjee, D.D. Dionysiou, S.C. Pillai,* Self-cleaning applications of TiO2 by photo-induced hydrophilicity and Photocatalysis, Applied Catalysis B: Environmental, **vol. 176–177**, 2015, pp. 396–428
[12] *A. Arunachalam, S. Dhanapandian, C. Manoharan, G. Sivakumar*, Physical properties of Zn doped TiO2 thin films with spray pyrolysis technique and its effects in antibacterial activity, Spectrochimica Acta Part A: Molecular and Biomolecular Spectroscopy, **vol. 138**, 2015, pp. 105–112
[13] *J.A. Byrne, B.R. Eggins, N.M.D. Brown, B. McKinney, M. Rouse*, Immobilisation of TiO2 powder for the treatment of polluted water, Applied Catalysis B: Environmental, **vol. 17**, 1998, pp. 25–36
[14] *P. Supphasrirongjaroen, P.W. Kongsuebchar, J. Panpranot, O. Mekasuwandumrong, C. Satayaprasert, P. Praserthdam,* Dependence of quenching process on the photocatalytic activity of solvothermal-derived TiO2 with various crystallite sizes, Industrial & Engineering Chemistry Research, **vol. 47**, 2008, pp. 693–697
[15] *J. Roszak, M. Stepnik, M. Nocun, M. Ferlinska, A. Smok-Pieniazek, J. Grobelny, E. Tomaszewska, W. Wasowicz, M. Cieslak*, A strategy for in vitro safety testing of nanotitania-modified textile products, Journal of Hazardous Materials, **vol. 256– 257**, 2013, 67– 75
[16] *R. Fagan, D.E. McCormack, D.D. Dionysiou, S.C. Pillai*, A review of solar and visible light active TiO2 photocatalysis for treating bacteria, cyanotoxins and contaminants of emerging concern, Materials Science in Semiconductor Processing, doi:10.1016/j.mssp.2015.07.052
[17] *Sammy W.Verbruggen*, TiO2 photocatalysis for the degradation of pollutants in gas phase: From morphological design to plasmonic enhancement, Journal of Photochemistry and Photobiology C: Photochemistry Reviews, **vol. 24**, 2015, pp. 64–82
[18] *A. Fujishima, X. Zhang, D.A. Tryk*, TiO2 photocatalysis and related surface phenomena, Surface Science Reports, **vol. 63**, 2008, pp. 515-582
[19] *J. Zhao, W. Xing, Y. Li, K. Lu*, Solvothermal synthesis and visible light absorption of anatase TiO2, Materials Letters, **vol. 145**, 2015, pp. 332–335
[20] *O.R. Vasile, E. Andronescu, C. Ghitulica, B.S. Vasile, O. Oprea, E. Vasile, R. Trusca,* Synthesis and characterization of nanostructured zinc oxide particles synthesized by the pyrosol method, Journal of Nanoparticles Research, **vol. 14**, 2012, pp. 1-13

[21] *L.G. Bettini, M.V. Dozzi, F.D. Foglia, G.L. Chiarello, E. Selli, C. Lenardi, P. Piseri, P. Milani,* Mixed-phase nanocrystalline TiO2 photocatalysts produced by flame spray pyrolysis, Applied Catalysis B: Environmental, **vol. 178**, 2015, pp. 226–232

[22] *A.B. Haugen, I. Kumakiri, C. Simon, M. Einarsrud,* TiO2, TiO2/Ag and TiO2/Au photocatalysts prepared by spray pyrolysis, Journal of the European Ceramic Society, **vol. 31**, 2011, pp. 291–298

[23] *H.M.N. Bandara, R.M.G. Rajapakse, K. Murakami, G.R.R.A. Kumara, G. Anuradha Sepalage*, Dye-sensitized solar cell based on optically transparent TiO2 nanocrystalline electrode prepared by atomized spray pyrolysis technique, Electrochimica Acta, **vol. 56**, 2011, pp. 9159– 9161

[24] *C. Chaisuk, A. Wehatoranawee, S. Preampiyawat, S. Netiphat, A. Shotipruk, J. Panpranot, B. Jongsomjit, O. Mekasuwandumrong*, Preparation and characterization of CeO2/TiO2 nanoparticles by flame spray pyrolysis, Ceramics International, **vol. 37**, 2011, pp. 1459–1463

[25] *T. Matsubara, Y. Suzuki, S. Tohno,* Synthesis and characterization of TiO2 powders by the double-nozzle electrospray pyrolysis method. Part 1. Refinement and monodispersion of sprayed droplets, C. R. Chimie, **vol. 16**, 2013, pp. 244–251

[26] *I.O. Acik, A. Junolainen, V. Mikli, M. Danilson, M. Krunks,* Growth of ultra-thin TiO2 films by spray pyrolysis on different substrates, Applied Surface Science, **vol. 256**, 2009, pp. 1391–1394

[27] *I.O. Acik, N.G. Oyekoya, A.Mere, A. Loot, L. Dolgov, V.Mikli, M. Krunks, I. Sildos,* Plasmonic TiO2:Au composite layers deposited in situ by chemical spray pyrolysis, Surface & Coatings Technology, **vol. 271**, 2015, pp. 27–31

[28] *F. Dufour, S. Pigeot-Remy, O. Durupthy, S. Cassaignon, V. Ruaux, S. Torelli, L. Mariey, F. Maugé, C. Chanéac,* Morphological control of TiO2 anatase nanoparticles: What is the good surface property to obtain efficient photocatalysts? Applied Catalysis B: Environmental, **vol. 174–175**, 2015, pp. 350–360

[29] *Z. Qiaoxin, L. Hao, W. Xiaohui, S. Xiaoliang, D. Xinglong*, Fabrication and characterization of nanosilver powder prepared by spray pyrolysis, Journal of Wuhan University of Technology-Mater, Sci. Ed. **vol. 24,** 2009, pp. 871-874

[30] *R. Nagarajan, T.A. Hatton*, Nanoparticles: Synthesis, Stabilization, Passivation, and Functionalization, American Chemical Society, 2008, ISBN 13: 9780841269699

[31] *C. Ghitulica, M. Cernea, B.S. Vasile, E. Andronescu, O.R. Vasile, C. Dragoi, R. Trusca*, Structural and electrical properties of NBT-BT0.08 ceramic prepared by the pyrosol method, Ceramics International, **vol. 39**, 2013, pp. 5925–5930

[32] *B.S. Vasile, O.R. Vasile, C. Ghitulica, E. Andronescu, R. Dobranis, E. Dinu, R. Trusca,* Yttria totally stabilized zirconia nanoparticles obtained through the pyrosol method**,** Physica Status Solidi A 207, **vol. 11**, 2010, pp. 2499–2504

[33] *T.E. Weirich, M. Winterer, S. Seifried, H. Hahn, H. Fuess,* Rietveld analysis of electron powder diffraction data from nanocrystalline anatase, TiO2, Ultramicroscopy, **vol. 81**, no. 3-4, 2000, pp. 263-270

[34] *H. Zhou, H. Alves, D. M. Hofmann, B. K. Meyer, G. Kaczmarczyk, A. Hoffmann, C. Thomsen*, Effect of the (OH) Surface Capping on ZnO Quantum Dots, Physica Status Solidi (b), **vol. 229,** no. 2, pp. 825–828

[35] *D. Jiang, L. Cao, G. Su, H. Qu, D. Sun*, Luminescence enhancement of Mn doped ZnS nanocrystals passivated with zinc hydroxide, Applied Surface Science, **vol. 253,** 2007, pp. 9330–9335

[36] *L. Peng, Y. Wang*, Effects of the template composition and coating on the photoluminescence properties of ZnS: Mn nanoparticles, Nanoscale Res Lett, **vol. 5,** 2010, pp. 839–845